Electronic Supplementary Material (ESI) for Journal of Materials Chemistry A.

Supporting Information

Lithium ion conductivity in Li_2S-P_2S_5 glasses – Building units and local structure evolution during the crystallization of superionic conductors Li_3PS_4, $Li_7P_3S_{11}$ and $Li_4P_2S_7$

Christian Dietrich[a], Dominik A. Weber[a], Stefan J. Sedlmaier[b], Sylvio Indris[c], Sean Culver[a], Dirk Walter[d], Jürgen Janek*[a,b], Wolfgang G. Zeier*[a]

[a]*Institute of Physical Chemistry, Justus-Liebig-University Giessen, Heinrich-Buff-Ring, 17, D-35392 Giessen, Germany.*

[b]*BELLA – Batteries and Electrochemistry Laboratory, Institute of Nanotechnology, Karlsruhe Institute of Technology, Hermann-von-Helmholtz Platz 1, D-76344 Eggenstein-Leopoldshafen, Germany*

[c]*Institute for Applied Materials, Karlsruhe Institute of Technology, Hermann-von-Helmholtz Platz 1, D-76344 Eggenstein-Leopoldshafen, Germany*

[d]*Institute of Occupational Medicine, Laboratories of Chemistry and Physics Justus-Liebig-University Giessen/University Hospital Giessen/Marburg, Aulweg 129, D-35392 Giessen, Germany*

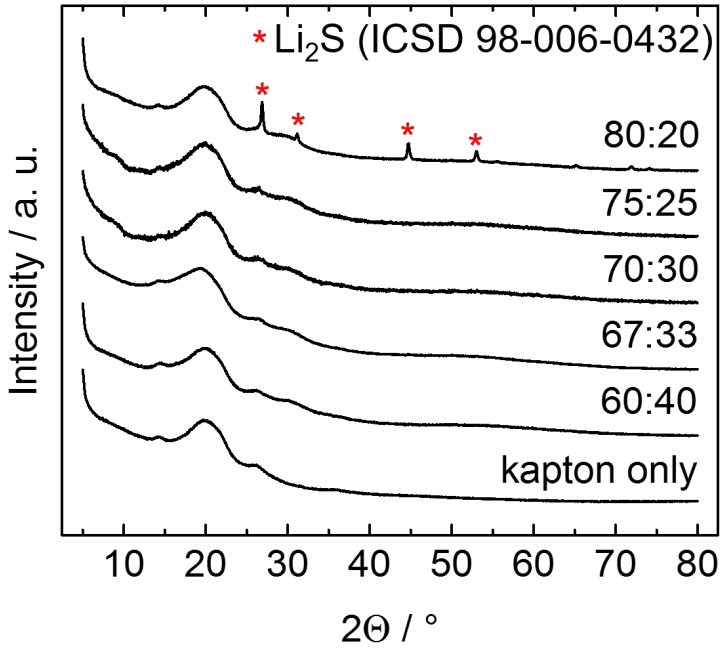

Figure S1: Laboratory X-Ray Diffraction Bragg data of LPS glasses. Only a broad background which is attributed to the polyimide cover foil (Kapton®) is observed for glasses with up to 75-mol% of Li_2S. 80:20 LPS glass shows visual reflections of crystalline Li_2S, which is not incorporated in the amorphous phase.

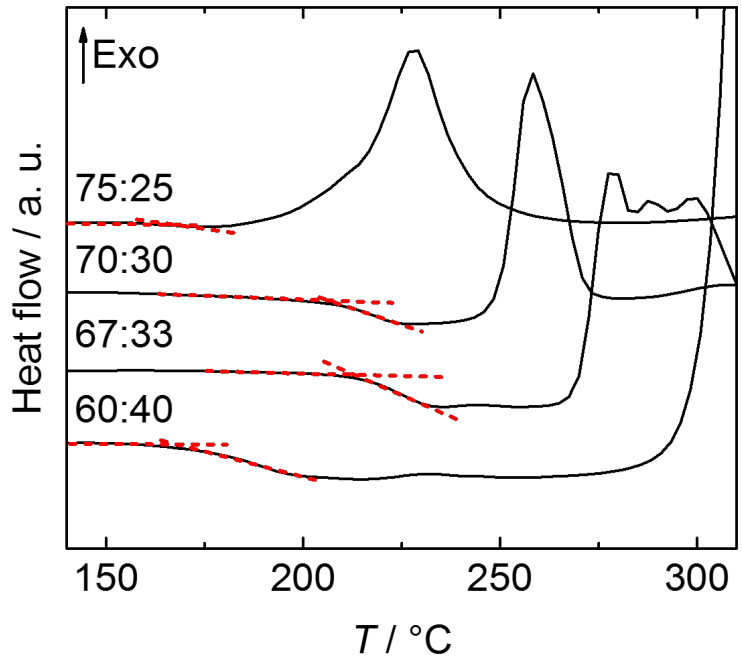

Figure S2: DSC curves of LPS glasses in closed Al crucibles with a heating rate of 20 $K \cdot min^{-1}$, baselines are marked for the determination of the glass transition. Glass transition of LPS glasses appears between 160 and 210 °C, while the crystallization takes place between 210 and 300 °C (see table S2).

Table S1: Results of peak deconvolution of Raman (80% Lorentzian and 20% Gaussian product functions) and NMR (Gaussian product function) spectroscopy.

		Raman			NMR		
$Li_2S:P_2S_5$		peak / cm^{-1}	FWHM / cm^{-1}	area / %	peak / ppm	FWHM / ppm	area / %
60:40	PS_4^{3-}	-	-	-	-	-	-
	$P_2S_7^{4-}$	402.2	25.0	77.8	90.3	19.0	81.6
	$P_2S_6^{4-}$	386.7	20.4	18.0	105.0	12.2	8.2
	PS_3^-	426.2	10.0	4.2	121.7	20.0	10.2
67:33	PS_4^{3-}	421.4	11.6	6.2	83.1	11.6	7.3
	$P_2S_7^{4-}$	405.3	19.4	81.9	90.3	14.0	78.5
	$P_2S_6^{4-}$	386.7	22.6	11.9	105.0	12.2	14.2
	PS_3^-	-	-	-	-	-	-
70:30	PS_4^{3-}	420.6	6.8	25.4	83.2	9.0	28.5
	$P_2S_7^{4-}$	406.6	20.0	69.4	90.7	14.4	58.6
	$P_2S_6^{4-}$	386.4	21.9	5.2	105.0	11.0	12.9
	PS_3^-	-	-	-	-	-	-
75:25	PS_4^{3-}	421.7	13.6	87.4	83.1	8.2	73.6
	$P_2S_7^{4-}$	404.5	21.0	4.1	91.2	5.3	12.6
	$P_2S_6^{4-}$	386.7	18.2	8.5	105.0	5.5	13.8
	PS_3^-	-	-	-	-	-	-
80:20	PS_4^{3-}	421.7	13.6	88.0	83.2	8.6	82.4
	$P_2S_7^{4-}$	-	-	-	90.1	13.7	7.4
	$P_2S_6^{4-}$	386.8	21.2	12.0	106.3	8.8	10.2
	PS_3^-	-	-	-	-	-	-

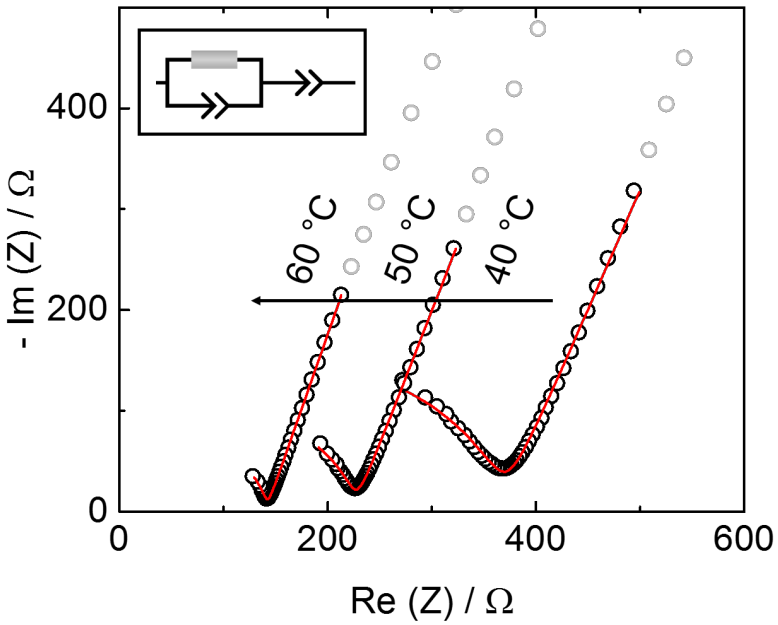

Figure S3: Temperature dependent impedance measurement of 80:20 LPS phase separated glass in Nyquist presentation. High frequency impedance data are represented in the complex plane by a single semicircle, which can be resolved for frequencies up to 7 MHz, and a straight line, strongly suggesting that the conductivity is predominantly ionic. The equivalent circuit (inset), which was used to obtain the activation energy of Li^+ transport, comprises a RQ element for lithium transport in the phase separated glass and a constant phase element representing the ionic adsorption and charge transfer between LPS and the blocking stainless steel electrodes. Fitting of impedance data is shown in the frequency range of 7 MHz to 12.5 kHz (solid red line).

Table S2: Electrochemical and physical properties of LPS glasses: lithium conductivity at room temperature σ_{25}; activation energy E_a; glass transition T_{glass} and first crystallization temperature T_{cry}.

Li_2S:P_2S_5	σ_{25} / S· cm^{-1}	E_a / kJ· mol^{-1}	E_a / meV	T_{glass} / °C	T_{cry} / °C
60:40	3.24E-06	50.7	525	167	298
67:33	3.78E-05	42.3	438	212	269
70:30	3.68E-05	43.5	451	207	249
75:25	2.76E-04	38.5	399	165	210
80:20	1.31E-04	42.3	439	-	-

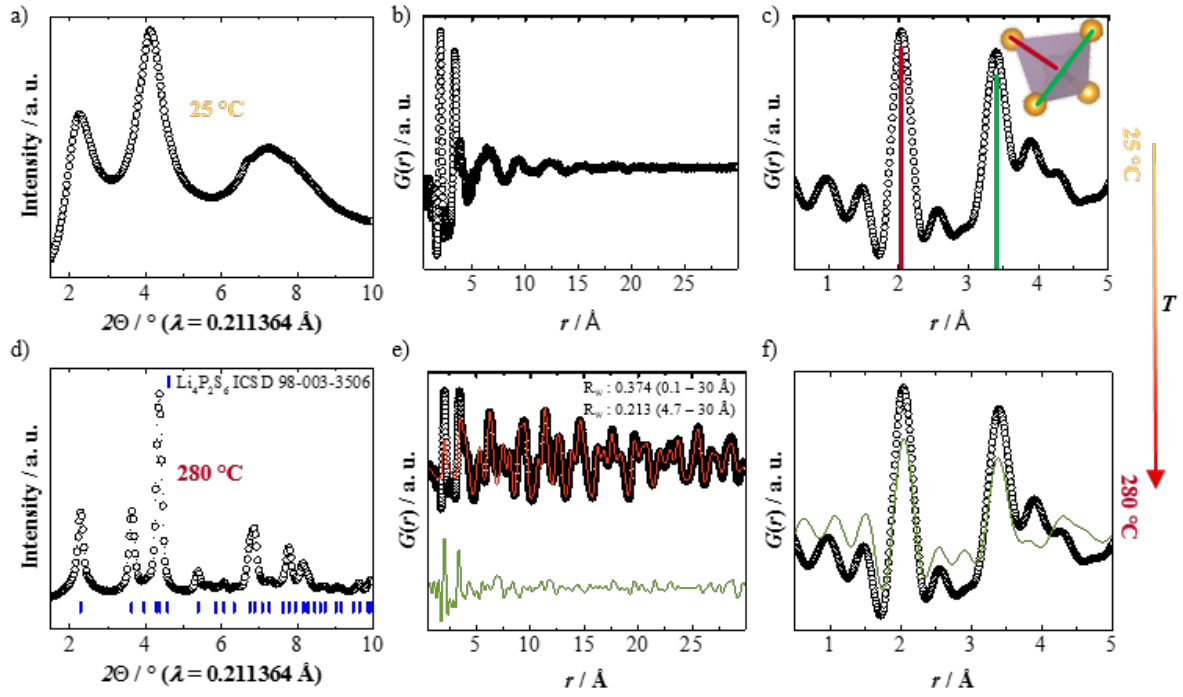

Figure S4: The observed synchrotron diffraction Bragg data of 60:40 LPS glass at room temperature only show a diffuse pattern, absent of any long-range order (a). No intense peaks for r > 4.7 Å are observed in the corresponding pair distribution function (b). The short-range order is determined by the PS_4-tetrahedral first coordination sphere, which is very similar for all LPS glasses (c). At 280 °C, reflections occur in the diffraction pattern (d), which could be assigned to $Li_4P_2S_6$ as the major phase and traces of Li_3PS_4. The fit (red line) of the resulting PDF data (black points) was based > 90 % on $Li_4P_2S_6$ (e). The resulting profile difference (green line) was compared with the room temperature PDF data of the initial glass in the range of 0.5 Å > r > 5 Å, which proof the coexistence of amorphous and crystalline phases, which is typical for LPS glass-ceramics (f).

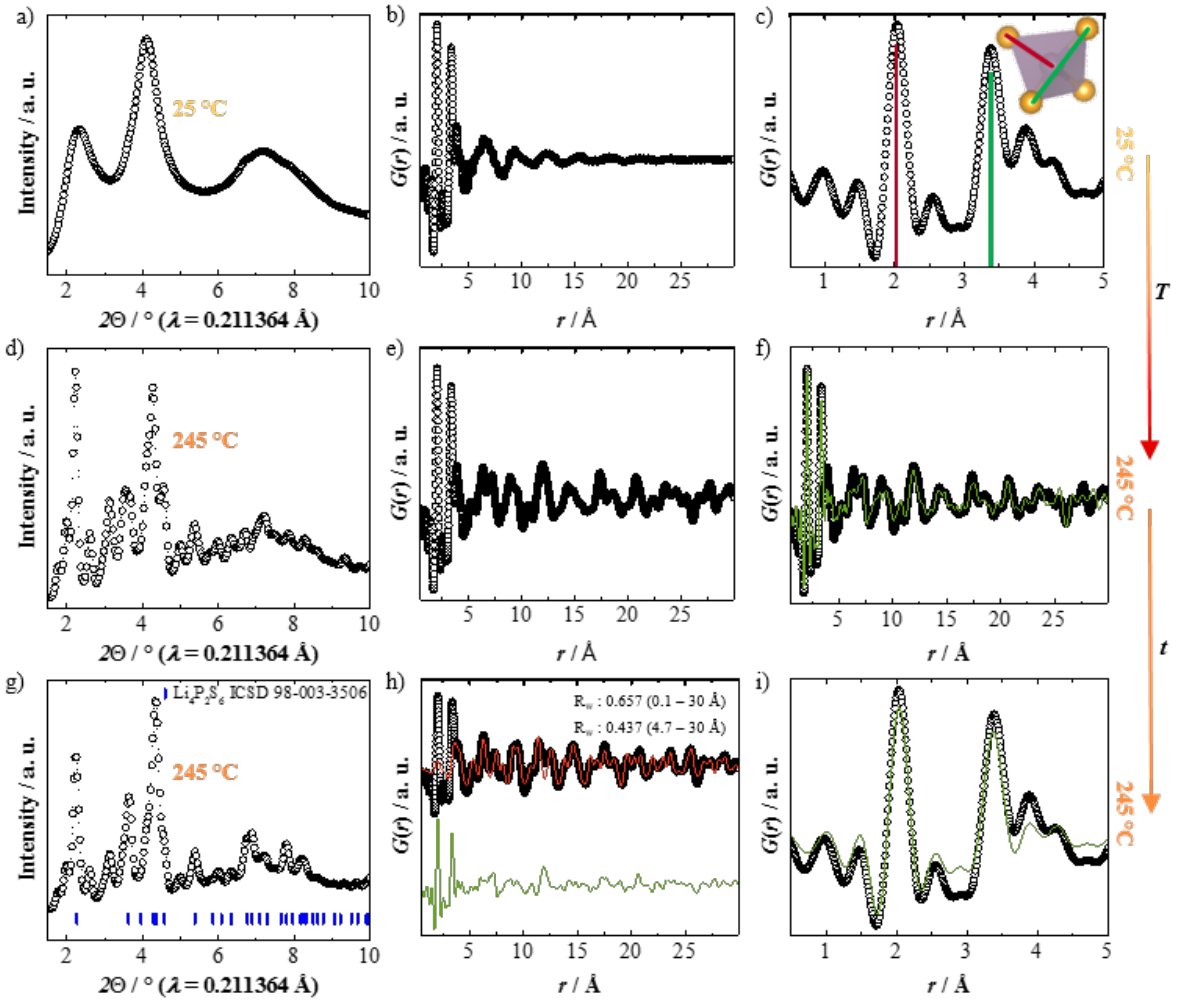

Figure S5: The observed synchrotron diffraction Bragg data of 67:33 LPS glass at room temperature only show a diffuse pattern, absent of any long-range order (a). No intense peaks for r > 4.7 Å are observed in the corresponding pair distribution function (b). The short-range order is determined by the PS_4-tetrahedral first coordination sphere, which is very similar for all LPS glasses (c). At 245 °C reflections are observed in the diffraction pattern (d), which lead to signals up to r = 30 Å in the corresponding PDF (e). This new phase could not be assigned to any known LPS structure. At the same temperature, this phase transforms to $Li_4P_2S_6$ (g). The corresponding PDF data (black line) was simulated with $Li_4P_2S_6$ (red line), which leads to some residue (high R_w) (h). The resulting profile difference (green line) was compared with the former unknown crystalline phase, which shows that the former phase is not completely converted (e). We cannot proof the full conversion at higher temperatures, as the capillary broke after this measurement. The resulting profile difference (green line) is also compared with the room temperature PDF data of the initial glass in the range of 0.5 Å < r < 5 Å (i). Although the crystal structure of the new phase is unknown, the strong signals corresponding to the PS_4-polyhedral first coordination sphere suggest the coexistence of amorphous and crystalline phases for the new phase as well as $Li_4P_2S_6$, which we found for all LPS glass-ceramics.

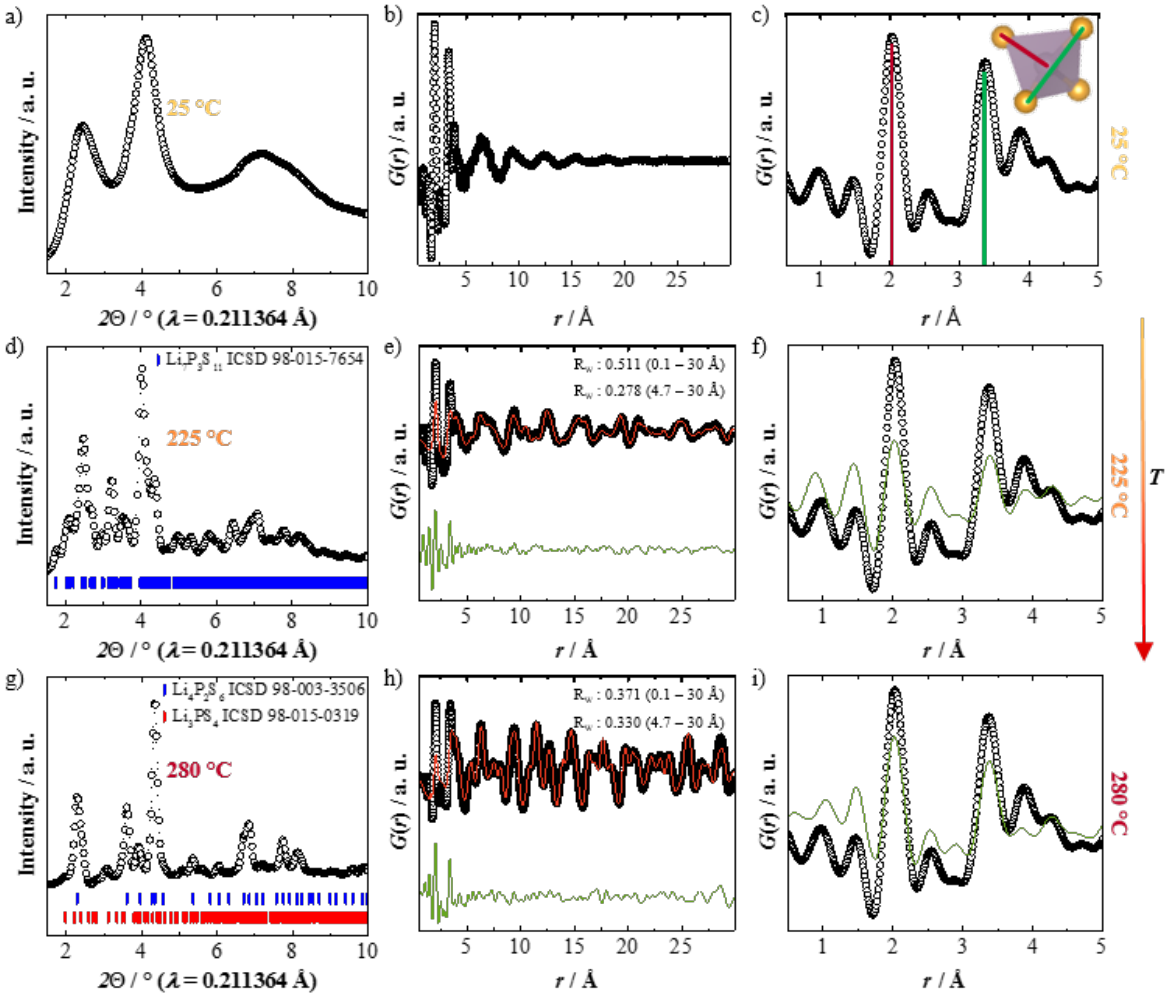

Figure S6: The observed synchrotron diffraction Bragg data of 70:30 LPS glass at room temperature show a diffuse pattern, absent of long-range order (a). No intense peaks for r > 4.7 Å are observed in the corresponding pair distribution function (b). The short-range order is determined by the PS_4-tetrahedral first coordination sphere, which is very similar for all LPS glasses (c). At 225 °C reflections occur in the diffraction pattern (d), which could be assigned to $Li_7P_3S_{11}$. The corresponding PDF data (black points) were simulated with $Li_7P_3S_{11}$ (red line) (e). Reflections at 280 °C could be assigned to $Li_4P_2S_6$ and Li_3PS_4 (g), which were used for the simulation of the PDF profiles (red line, h). The resulting profile differences of the PDF fitting at 225 °C (f) and 280 °C (i) were compared with the room temperature PDF data of the initial glass in the range of 0.5 Å > r > 5 Å, which corroborate the coexistence of amorphous and crystalline phases.